Materials Science & Engineering A 679 (2017) 1–6

Contents lists available at ScienceDirect

Materials Science & Engineering A

journal homepage: www.elsevier.com/locate/msea

In situ observation of the "crystalline⇒amorphous state" phase transformation in Ti_2NiCu upon high-pressure torsion

R.V. Sundeev[a,*], A.V. Shalimova[b], A.M. Glezer[b,c], E.A. Pechina[d], M.V. Gorshenkov[c], G.I. Nosova[b]

[a] Moscow Technological University, "MIREA", Vernadskogo pr. 78, 119454 Moscow, Russia
[b] I.P. Bardin Science Institute for Ferrous Metallurgy, Radio st. 23/9, 105005 Moscow, Russia
[c] National University of Science and Technology "MISIS", Leninskii pr. 4, 119049 Moscow, Russia
[d] Physical-Technical Institute Ural Branch RAN, Kirov st. 132, 426000 Izhevsk, Russia

ARTICLE INFO

Keywords:
Severe plastic deformation
High pressure torsion
Amorphous materials
Phase transformation
Amorphization

ABSTRACT

The evolution of the structure and mechanical behavior upon deformation has been studied experimentally *in situ* by room-temperature high-pressure torsion (HPT) of the initially crystalline Ti_2NiCu alloy. An abrupt increase in the shear stress upon HPT has been revealed. It was found that the observed effect is due to the deformation-induced "crystalline⇒amorphous state" phase transformation and the corresponding change in the mechanism of severe plastic deformation. It is shown that the amorphization of the material begins at the boundaries of grains and fragments of the crystalline phase as a result of grain boundary sliding processes. It was established that the amorphous boundaries form a "grain-boundary framework", which upon deformation is expanded and transformed into bulk amorphous phase.

1. Introduction

The structural and thermodynamic aspects of the process of deformation-induced amorphization and deformation-induced crystallization occurring upon severe plastic deformation (SPD) are widely studied in recent years and are the matter of considerable debate [1–7]. Generally, this process is developed in amorphizable multicomponent Pd-Cu, Ti-Zr, Zr-Cu, Mg-Cu, Ti-Ni, and Fe-B based metallic systems. Since the end of the last century, the deformation-induced amorphization was intensely studied upon high-pressure torsion (HPT). The TiNi based alloys were investigated most actively [8–12].

The structural changes in the T-50.5 at% Ni alloy were first studied in [12] upon HPT, and a possible scheme of the transformation of crystalline structure to the amorphous state has been proposed. It was suggested that the amorphization begins at the boundaries of "rotating" nanocrystals. The structural characteristics of the transition of the $Ni_{50}Ti_{30}Hf_{20}$, $Ti_{50}Ni_{25}Cu_{25}$, $Zr_{50}Ni_{18}Ti_{17}Cu_{15}$, and $Fe_{78}B_{8.5}Si_9P_{4.5}$ crystalline alloys into amorphous state upon HPT were experimentally studied in [2]. It was shown that crystalline alloys of different compositions substantially differ in amorphization ability, which is determined by the additive abilities to deformation-induced amorphization of individual crystalline phases contained in the alloy. It also follows from [2] that the crystalline alloys coinciding in chemical composition with the corresponding amorphous phase almost completely transform into amorphous state. At a general understanding of the direction, in which the structure of crystalline alloys evolves upon HPT, the important details necessary to clarify the specific structural mechanism of deformation-induced amorphization remain unclear. In addition, such study could substantially help to understand general SPD regularities, the physics of which is far from understanding.

Unfortunately, the transition from crystalline to amorphous state up until now failed to be detected *in situ* directly upon SPD by recording power parameters in the "stress - strain" deformation curve since, upon HPT, such detection requires continuous and precise registration of the torsion force (torsional moment) upon deformation. Meanwhile, deformation upon HPT is extremely nonuniform over the sample volume, and this naturally leads to the heterogeneity of structural states. We showed this experimentally by local X-ray diffraction examination with synchrotron radiation in seven points of a sample of 8 mm in diameter [13].

With reference to the above mentioned, the aim of this work was a detailed study and analysis of the structure evolution in the Ti_2NiCu crystalline samples by comparing the power deformation parameters recorded *in situ* upon HPT with the results of the structure examination after unloading the sample at different deformation stages. Such study should clarify, *where and how* does the amorphous phase occur upon HPT of crystalline material.

* Corresponding author.
E-mail address: apricisvir@gmail.com (R.V. Sundeev).

http://dx.doi.org/10.1016/j.msea.2016.10.028
Received 17 September 2016; Received in revised form 7 October 2016; Accepted 8 October 2016
Available online 11 October 2016

2. Experimental

The Ti_2NiCu alloy was taken for the study. Two structural states of the material, completely amorphous and completely crystalline, were studied. The amorphous state was prepared by melt quenching in vacuum at a cooling rate of 10^6 °C/sec as ribbons about 50 μm thick and 8 mm wide. The crystalline samples were obtained by annealing of the initial ribbon at 500 °C for 30 min. For continuous registration of torsional moment upon room-temperature HPT, the Ti_2NiCu samples were tested in two structural states with a modernized setup [14] using a force sensor consisting of two symmetrically arranged additional elastic elements with serial connection of heat resistors into a bridge circuit for measuring the torsional moment. Such system allowed us to eliminate random errors arising from incorrect installation of the sample and the movable anvil. The relative error of torsional moment measurement and the sensor calibration is not more than ± 2%. The shear stress (σ) was calculated by the formula [15]:

$$\sigma = 3M/2\pi r^3, \quad (1)$$

where M is the torsional moment and r is the radius of the gage area on the assumption that the average stress $\sigma(n)$ is constant along the sample radius.

The samples were deformed at a constant quasi-hydrostatic pressure of 6 GPa at room temperature, the rotation rate of the movable anvil was 0.67 rpm, and the degree of deformation n =6–8, where n is the number of revolutions of the movable anvil. Note: interval of hydrostatic pressure eliminating slippage of samples for Ti_2NiCu material amounts 4–8 GPa, which follows from the works [16,17]. The structure was examined by transmission electron microscopy (TEM) with a JEOL JEM 1400 microscope at an accelerating voltage of 160 and 200 kV. The structure was also examined by high-resolution transmission electron microscopy (HRTEM) with a Titan 80–300 transmission electron microscope with probe-spherical aberration corrector at 300 kV at a resolution of 0.079 nm. The samples of 3 mm diameter for electron microscopic examination were cut in the middle of the radius of the deformed samples. The fraction of the crystalline phase (V) was calculated by X-ray diffraction (XRD) data [18] taken by the step-by-step Bragg-Brentano method in CoKα radiation with a graphite monochromator on the diffracted beam. The error in determining the crystalline phase fraction was about 10% in the presence of a sufficient number of crystalline phase reflections in the spectrum.

3. Results and discussion

Fig. 1 shows the curves of continuously changing shear stress $\sigma(n)$ in accordance with Eq. (1) upon room-temperature HPT for initially crystalline (curve 1) and initially amorphous (curve 2) Ti_2NiCu alloy. For comparison, Fig. 1 also shows curve 3 of continuously changing shear stresses $\sigma(n)$ for polycrystalline copper, which does not undergo any phase transformations upon HPT. Curve 1 exhibits an abrupt, almost two-fold increase in the flow stress $\sigma(n)$ in a strain range of n =2–4. This can be qualified as deformation-induced phase transformation. It is important to emphasize that the deformation curve 1 at $n \geq 4$ is similar is character to curve 2 corresponding to the initial amorphous state of the alloy. Moreover, the maximum shear stress σ_{max} at $n \geq 4$ for deformation curves 1 and 2 (points A and A′, respectively) are identical (580 MPa). This gives us every reason to believe that the anomalous increase in $\sigma(n)$ in curve 1 at n =2–4 is caused by the transition of the initially crystalline Ti_2NiCu alloy into the amorphous state. Curve 1 for the convenience of further consideration can be arbitrarily divided into 3 stages: the first SPD stage (n =0–2) is accompanied by a slight change in shear stress; at the second SPD stage (n =2–4) the level of shear stress increases drastically, from 350 to 580 MPa; finally, the third SPD stage ($n \geq 4$) represents a gradual decrease in shear stress, from 580 MPa to 450 MPa.

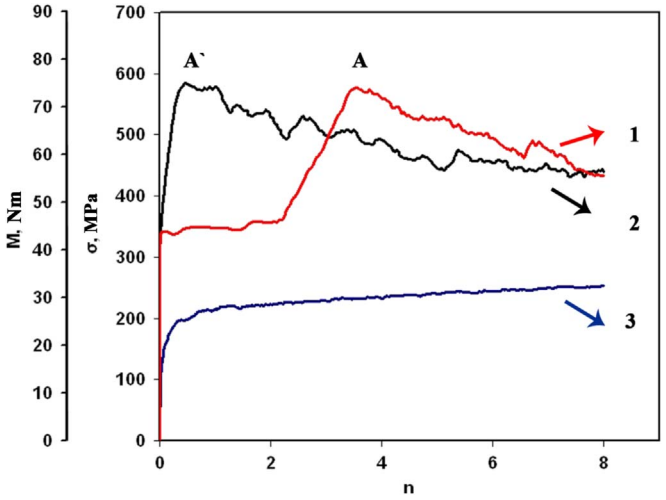

Fig. 1. The **M**(n) and σ (n) dependences: (1) initially crystalline Ti_2NiCu alloy, (2) initially amorphous Ti_2NiCu alloy, and (3) polycrystalline copper.

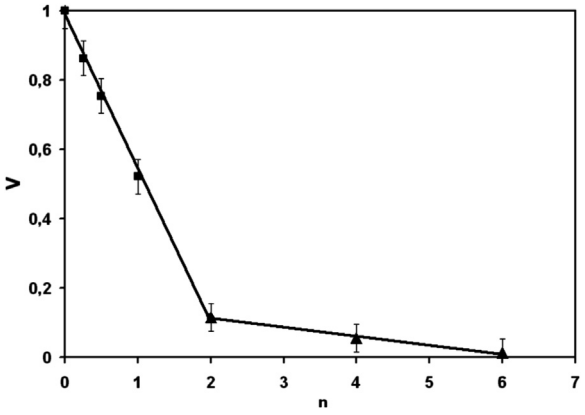

Fig. 2. Crystalline phase fraction V as a function of the degree of deformation n upon HPT of the crystalline Ti_2NiCu alloy (■ – XRD, ▲ – TEM).

Fig. 2 represents the crystalline phase fraction V calculated by XRD ($n < 2$) and TEM ($n \geq 2$) data corresponding to the structure of the initially crystalline Ti_2NiCu alloy after unloading at various stages of deformation upon HPT.

Comparison of the data given in Figs. 1 and 2 shows that the amorphization of the crystalline alloy at room temperature generally occurs at the first SPD stage corresponding to n =0–4: V decreases from 1 to 0.1. At the second SPD stage, there is a further very slight decrease in V to very low values (≈0.05). Next, the third SPD stage corresponds to complete structure amorphization within the error of electron-microscopic determination of V, and the plastic deformation of fully amorphous material occurs. Note that the experimental data obtained upon continuous record of torsional moment (Fig. 1) and the structural data (Fig. 2) obtained after unloading are quite comparable since, upon the transition of $\sigma(n)$ curve from the first SPD stage to the second one, the deformation curves 1 (initial crystalline state) and 2 (initial amorphous state) are similar in character, and V virtually corresponds to the completely amorphous state of the alloy.

The initial structure of the alloy in the crystalline state (Fig. 3a) consists of a complex mixture of the groups of B19 martensite plates formed upon cooling from a temperature of 500 °C at the boundaries of highly misoriented grains of the high-temperature B2 phase. The length of the B19 martensite plates observed in electron microscopic images varies widely from 500 to 2000 nm.

The first HPT stage (Fig. 1, curve 1) corresponds to the TEM images shown in Figs. 3–6 (n =1/4 and n =1/2). It is seen (Fig. 3b and c) that,